Article

Silica fume enhances the mechanical strength of alkali-activated slag/fly ash pastes subjected to elevated temperatures

Weidong Dai [a] and Yachao Wang [b] *

[a] Queshan County highway development center, Zhumadian 463200, Henan Province, PR China
[b] School of Resource Engineering, Xi'an University of Architecture & Technology, Xi'an 710055, PR China
* Correspondence: wangyachao@xauat.edu.cn

Abstract: The fireproof design of geopolymer has intriguing increasing attention by adjusting multi-component metallurgical solid wastes, due to its low-carbon emission, cost-effectiveness, and environmental conservation. Herein, the effects of silica fume (SF) on the microstructure and mechanical properties of alkali-activated slag/FA (fly ash) pastes subjected to elevated temperatures (150, 500, 850, and 1200℃) are investigated, to clarify the fact that whether or not the SF generates positive roles in mechanical strength of slag/FA (slag: FA=30:70, wt.%) geopolymers during building fires. The results show that the replacement of FA with 10 wt% SF (silica fume) promotes the increasing pore volume with a diameter of 0.2~3 μm, leading to an increase in the compressive or flexural strength below 850℃, "right shifts" of the endothermic peak, appearing uniform and compact fracture surfaces. Meanwhile, the gehlenite and labradorite generate after exposure above 850℃. While the bloating effect of the SF-containing sample occurs at 1200℃, leading to a greater deformation, due to the further restructuring of the amorphous geopolymer chain N-A-S-H or N-(Ca)-A-S-H composed from the $[SiO_4]^{4-}$ and $[AlO_4]^{5-}$. It explores an effective approach for improving geopolymer's fireproof performance by adjusting the solid-waste formulation.

Keywords: alkali-activated; silica fume; elevated temperatures; slag; fly ash

1. Introduction

Alkali-activated geopolymer binders are aluminosilicate inorganic polymers that have the advantages of high strength, good corrosion resistance, low carbon emission during production, and amorphous net-work structures, holding unique properties compared with Portland cement, such as reduced CO_2 emission, simple technological process, excellent durability, and reduced cost [1-2]. Currently, the building fire has been increasingly threatening the human settlement, as an alternative to cement, the geopolymer should undertake the fire at about 1000°C. Therefore, the fireproof design of geopolymer has intriguing increasing attention by adjusting multi-component metallurgical solid wastes [3].

Currently, the global perspective on burgeoning sustainability boosts the development of converting industrial by-products slag derived from blast furnace iron making and fly ash (FA) from coal-fired power plants into cementitious materials, which is very promising to develop solid waste-based pastes without heating curing at about 60 °C [4], due to the reactive calcium involved in slag. Investigations and wide applications of binary slag/FA geopolymers [5-7] have been hotspots to realize the recycling economy and environmental protection. Meanwhile, silica fume (SF) as an industrial by-product, also possesses an amorphous aluminosilicate nature, due to the more sodium alumino-silicate hydrate (N-A-S-H) network resulting in the increased compressive strength [8]. Theoretically, SF could trigger and enhance geopolymerization [9], presenting improved fire resistance, due to the thermally stable N-A-S-H, compared with the C-S-H in cement.

 doi:10.20944/preprints202305.2244.v1

Meanwhile, the excellent heat resistance of binary slag/FA geopolymers has been manifested in comparison to traditional Portland cement. Pavel et al. [10] describe the behavior and structural changes of the slag matrix during and after exposure to temperatures as high as 1200℃. The effect of elevated temperatures on the chemical stability and residual compressive strength of neat sodium sulfate-activated slag pastes is also reported [11]. However, the relative strength of the neat slag paste is superior to the counterpart incorporated SF, which exerts an adverse impact on the thermal shock resistance [12]. Therefore, whether or not the SF generates positive roles in binary slag/FA geopolymers needs to be clarified to develop multi-component SF/slag/FA binders with fireproof properties, especially for the performance under elevated temperatures corresponding to the building fire at about 1000°C.

Consequently, the review of the literature has indicated that few publications report the performance of SF involved in binary slag/FA pastes after exposure to elevated temperatures at about 1000°C. The primary purpose of this paper investigates the effects of SF on the microstructure of slag/FA binders after exposure to elevated temperatures, which are activated by sodium silicate solution with the SF: slag: FA ratio of 10: 30: 60 (wt.%)[13]. The characterizations contain the residual stresses, mass loss, shrinkage, mineral phase, heat flow, and morphology, with alkali-activated slag/FA (slag: FA=30:70, wt.%) binder without SF as a control. It explores the effect of SF on the mechanical strength of alkali-activated slag/fly ash pastes subjected to the elevated temperatures corresponding to the building fire, prompting the effective recycling approach for improving geopolymer's fireproof performance by adjusting the solid-waste formulation.

2. Material and methods

2.1. Raw materials

FA was obtained from the Hancheng power plant (Shan'Xi province) with Blaine specific surface area of 500 m^2/kg and a mean particle size of 11.2 μm after oven drying at 105°C and ball-milling for 1 h. Granulated ground blast furnace slag was obtained from Delong powder company with Blaine specific surface area of 420 m^2/kg and a mean particle size of 15.5μm. SF was collected from Linyuan company with Blaine specific surface area of 25 m^2/g and a mean particle size of 2.6 μm. The chemical compositions of raw materials are shown in Table 1. Alkali-activator, $Na_2SiO_3 \cdot 9H_2O$ (A.R.), was purchased from Tianjin Yaohua chemical reagent company.

Table 1. Chemical compositions of raw materials.

Raw materials	Mass percent (wt %)									
	CaO	SiO_2	Al_2O_3	Fe_2O_3	MgO	Na_2O	K_2O	SO_3	TiO_2	Loss
FA	3.82	55.18	31.19	5.07	0.60	0.29	1.99	0.28	1.05	0.53
Slag	39.65	31.29	14.31	0.61	8.51	0.63	0.58	2.94	0.83	0.54
SF	1.81	86.21	3.49	1.85	1.93	1.18	1.66	0.38	0.84	0.65

2.2. Preparation of specimens

The alkali-activated ternary SF/slag/FA pastes were synthesized by adding sodium silicate (15wt% $Na_2SiO_3 \cdot 9H_2O$) solution into the uniform mixture of FA, slag, and SF with a water/(SF+salg+FA) ratio of 0.3 to form the slurry in a cement mortar machine, the weight ratio of FA: slag: SF was 6:3:1[13], the binary specimen with a slag: FA ratio of 7:3 was used as a reference. The slurry was poured into the stainless triplet mold of 160×40×40 mm^3 and vibrated up and down for 60 s, which was demoulded after curing for one day and cured in a standard cement mortar curing box with a relative humidity of 90% at room temperature (RT) for 28 days.

2.3. Characterizations

 doi:10.20944/preprints202305.2244.v1

The mechanical strength of specimens was systematically tested including compressive and flexural strength, the specimens after curing 28d were exposed to elevated temperatures with an increment of 350℃ during 150-1200℃ and a heating rate of 5℃/min, maintaining 2h at various elevated temperatures of 150, 500, 850, and 1200℃, air-cooled to RT for evaluation, respectively. The 1200℃ is selected to correspond to a real building fire, and the duration of 2h corresponds to the fire endurance of ordinary cement, respectively.

Compressive strength was tested by a full-automatic cement mortar compressive testing machine of YAW-300 type with a pressurization rate of 2.4 kN/s, the error was 0.1 MPa. Flexural strength was measured by a motorized bending tester of DKZ-5000 type with an error of 0.03 MPa. The mechanical strength of specimens was conducted on 3 replicates, respectively, using the average value as the final result with a standard deviation <5%. Micro-morphology analysis of samples was conducted on a Quanta 200 scanning electron microscope (SEM) with a working condition of 20 *kV* voltage. The X-ray diffractometer (XRD, D/MAX-2200, Nippon Scientific Co., Ltd, China) is used to record XRD patterns of specimens using Cu Kα radiation.

Thermogravimetric analysis (TG) of Mettler was used to measure the mass loss and heat flow of specimens during the heating process of 50-950℃ under a nitrogen atmosphere at a heating rate of 30℃/min. Digital photos were shot by a Fujifilm AV100 camera. FTIR spectrum was measured using a spectrometer (FTIR-650) in absorption mode, the transmission of the IR beam is real-timely recorded, it was conducted in the range of 3000~500 cm^{-1} with a spectral resolution of 2 cm^{-1}, and samples were mixed with KBr with a sample/KBr weight ratio of 1/100. Pore size distributions of samples after 28 days of curing were tested by AUTOPORE 9500 mercury porosimetry under a nitrogen pressure of 0.3 MPa.

3. Results

3.1. XRD

XRD patterns of specimens after exposure to elevated temperatures are shown in Fig.1, it is noted that the patterns of SF-containing specimens are similar to that of specimens without SF, indicating no new mineral formed after incorporating SF at 150~500℃. Because the SF inherently belongs to amorphous silica without any crystallines, the triggered reactions only extend or crosslink the amorphous N–A–S–H chains. However, the Gehlenite as $Ca_2Al(AlSiO_7)$ (No. of JCPDS:98-000-0226) and labradorite as (Ca, Na)(Si, Al)$_4O_8$, (No. of JCPDS:98-000-0272) form as predominant mineral phase after 850℃ and 1200℃ treatment, it demonstrates that the exposure to 850℃ induces transformation of gehlenite and labradorite, which is further enhanced by the heating treatment of 1200℃, and the molar ratio of CaO/SiO_2 and Al_2O_3/SiO_2 decreases from gehlenite to labradorite, due to the activated silica participates in the reactions.

Meanwhile, there are the diffraction peaks of quartz (SiO_2, No. of JCPDS: 98-000-0369) and mullite ($Al_{4+2x}Si_{2-2x}O_{10-x}$(x~0.4), No. of JCPDS:98-000-0319) in XRD patterns of specimens after exposure to 850℃ and 1200℃, but their diffraction intensity of peaks significantly weaken. Bernardo et al.[14-15] demonstrate that the mixture of water glass/soda–lime–silica/clay, as well as a mixture of red mud/fly ash/porcelain stoneware tiles, could transform into labradorite with good mechanical strength after calcination. Segui et al. [16] suggest that labradorite grows into a binder composed of pozzolan, lime, and gypsum. Because kaolin clay promotes the formation of labradorite in glass–ceramics [17], Fang et al.[18] suggest the released CaO together with unreacted portlandite and gypsum, interacting with N–A–S–H to form labradorite after calcination at 1050℃. Therefore, it determines that activated CaO, Al_2O_3, and SiO_2 could transform into a labradorite after high-temperature treatment.

Preprints (www.preprints.org) | NOT PEER-REVIEWED | Posted: 31 May 2023 doi:10.20944/preprints202305.2244.v1

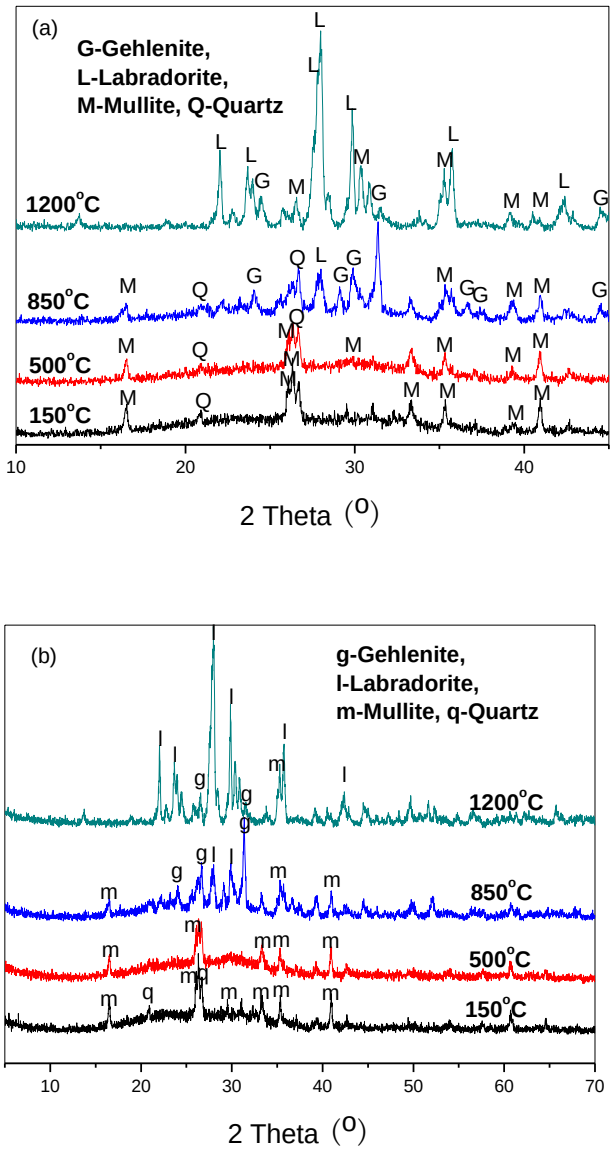

Figure 1. XRD of sample including (a) Slag/FA binders and (b)SF/ slag/FA binders.

Because the content of quartz in the fly ash of C type decreases on sintering above 850°C and transforms into new crystallite structures [19]. The finding of our research is in agreement with the report that gehlenite is drastically reduced as it starts to react with quartz towards wollastonite and anorthite at 1050 °C in the Fe_2O_3-SiO_2-Al_2O_3 clay [20]. Ding et al. [21] also assert that mullite and corundum of FA could dissolve and transform into calcium sodium hydrate silicate ($NaCaHSiO_4$). It confirms that quartz and mullite could transform into feldspar above 850°C in an alkali-activated binary slag/FA binder system.

3.2. Mechanical strength of specimens subjected to high temperatures

3.2.1. Residual stress of specimens

The residual stress of specimens exposed to elevated temperatures is shown in Fig.2, the SF-containing specimen displays higher mechanical performance than the specimen without SF, indicating that SF imparts a strengthening effect to the slag/FA binder, as well as after exposures to various elevated temperatures. The residual compressive strengths

 doi:10.20944/preprints202305.2244.v1

are improved after heat treatment of 150 and 500℃ compared with the specimen at RT, corresponding to 105.6 MPa (increased by 8.8%, 150℃) and 108.6 MPa (increased by 14.1%, 500℃) for the specimen incorporated SF. The ordinary cement is prone to disintegrate and collapse at about 600℃ [22], due to the dehydration or decomposition of calcium silicate hydrate. While the slag/FA geopolymer exhibits improved mechanical strength, corresponding to enhanced fire resistance.

Given the decomposition [22] of N-(C)-A-S-H or C-A-S-H after 850℃ treatment, appearing a rapid decline of residual stress for the both two specimens. However, the flexural strength of the SF-containing specimen after 1200℃ treatment climbs to 5.6 MPa sharply, while that of the specimen without SF is only 1.1 MPa, which might be attributed to the transformation of labradorite combined with the XRD results.

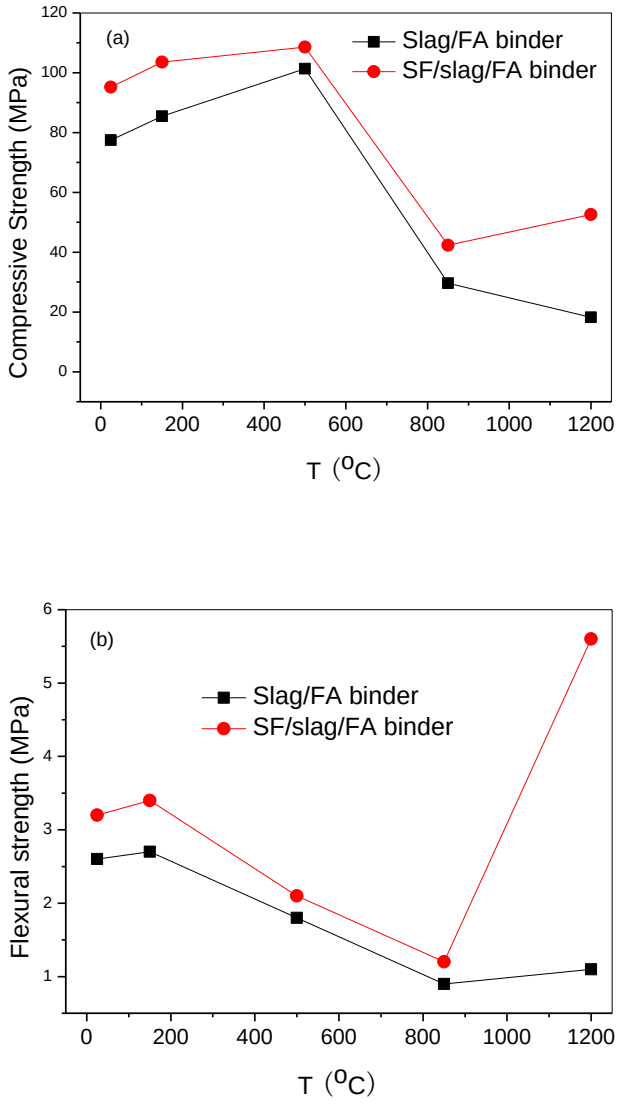

Figure 2. Mechanical strength of specimens subjected to high temperatures including (a) Compressive strength and (b) Flexural strength.

3.2.2. Deformation

The mass loss of specimens and volume shrinkage of specimens are displayed in Fig.3. Regarding the SF-containing specimen, higher stability presents under sub-high

 doi:10.20944/preprints202305.2244.v1

temperatures while greater mass loss and shrinkage are observed under high temperatures. The shrinkage approaches 6.9% at 500℃, 8.6% at 850℃, and 9.4% at 1200℃, implying that the replacement with 10 wt% SF triggers more volume deformation under higher temperatures, compared with the control without SF. Because the as-formed N-A-S-H derived from the incorporated SF and the unreacted SF hold high reactivity, which is prone to melt and trigger silicate reactions.

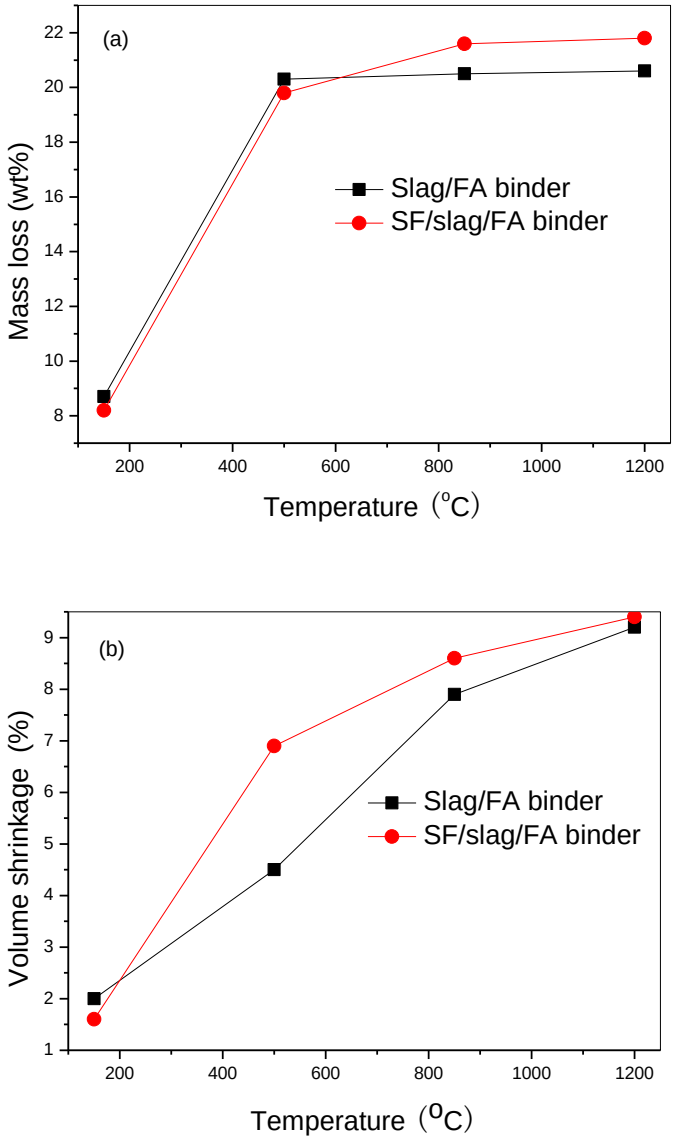

Figure 3. Deformation of specimens after exposure to elevated temperatures, including (a) Mass loss and (b) Volume shrinkage.

3.3. Morphology and Microstructure

3.3.1. Macro-morphologies

 doi:10.20944/preprints202305.2244.v1

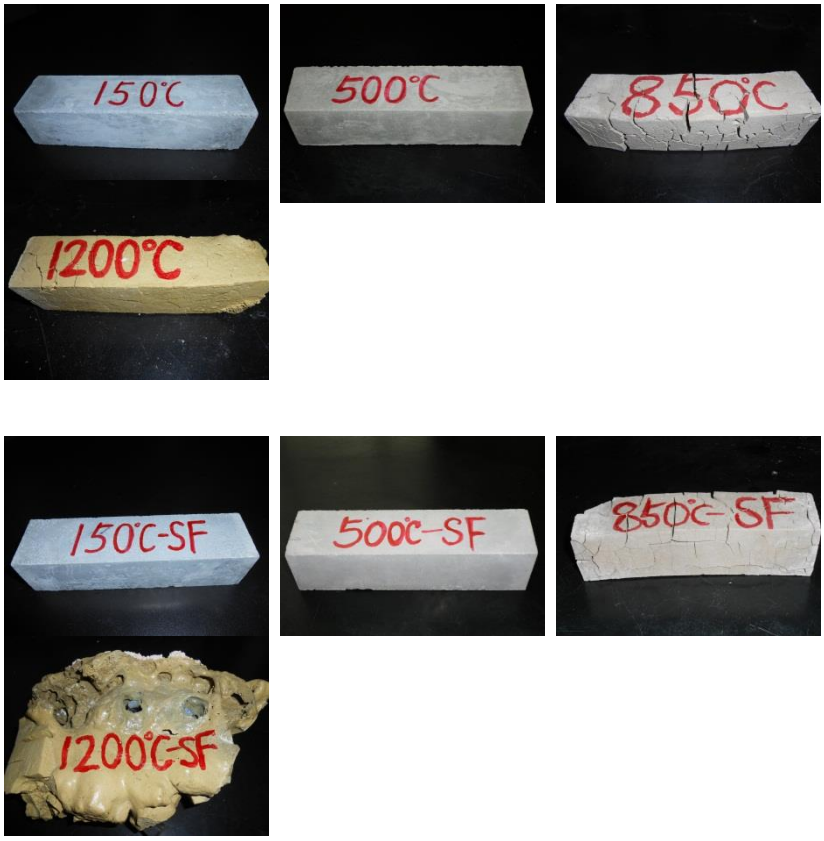

Figure 4. Apparent morphology of binders after heat treatment.

The color change of pastes is shown in Fig.4, the gray surface gradually transforms into yellow with increasing cracks, and the volume of specimens exhibits slight shrinkage in their dimensions continuously with the increasing heat treatment temperatures. The higher temperature causes bigger cracks as shown in Fig.4, due to the thermal stress from the various swelling coefficients within the geopolymer. However, the SF-containing specimens display fewer and shallower cracks in comparison to specimens without SF, especially after the treatment of 850°C, corresponding to the higher strength. Generally, the incorporated SF favors enhancing the mechanical strength of slag/FA binder from RT to 850°C, evidenced by the improved strength, which is also favorable to undertaking the building fire.

However, the obvious melting is observed for the SF-containing specimen subjected to 1200°C, which is disadvantageous to undertaking the building fire effectively. Therefore, the bloating effect on the dimension for SF-containing specimens occurs after exposure to 1200°C, while specimens without SF keep the initial shape, revealing the reduced melting point of slag/FA binders incorporated by SF.

3.3.2. Micro-morphologies

The micro-morphologies of specimens subjected to elevated temperatures are presented as a series of electron micrographs with an amplification of 5000× in Fig.5-6. The coexistence of the amorphous silicate gels and crystals is observed, but unreacted spherical FA particles disappear and the rod-like or needle-like feldspar increases with the increasing treatment temperatures gradually, due to the further geopolymerations. Generally, uniform and smooth fracture surfaces with smaller holes are observed for ternary SF/slag/FA binder (Fig.6a-c) after sub-high temperature (500 °C) exposure in comparison to the binary specimen with the rugged and non-uniform surface (Fig.5a-c). Interestingly, more and larger pores or holes appear on the fracture surface of specimens after 850 °C heating as shown in Fig.5d, which shrink for SF-containing specimens as shown in Fig.6d.

Preprints (www.preprints.org) | NOT PEER-REVIEWED | Posted: 31 May 2023 doi:10.20944/preprints202305.2244.v1

Compared with the needle-like feldspars in Fig.5e, the SF-containing sample exhibits a compact and dense structure after exposure to 1200 °C, the needle-like feldspars are covered or embedded by the uniform and amorphous silicates as shown in Fig.6e, revealing that the doped SF effectively inhibits the cracking and facilitates densification to some extent.

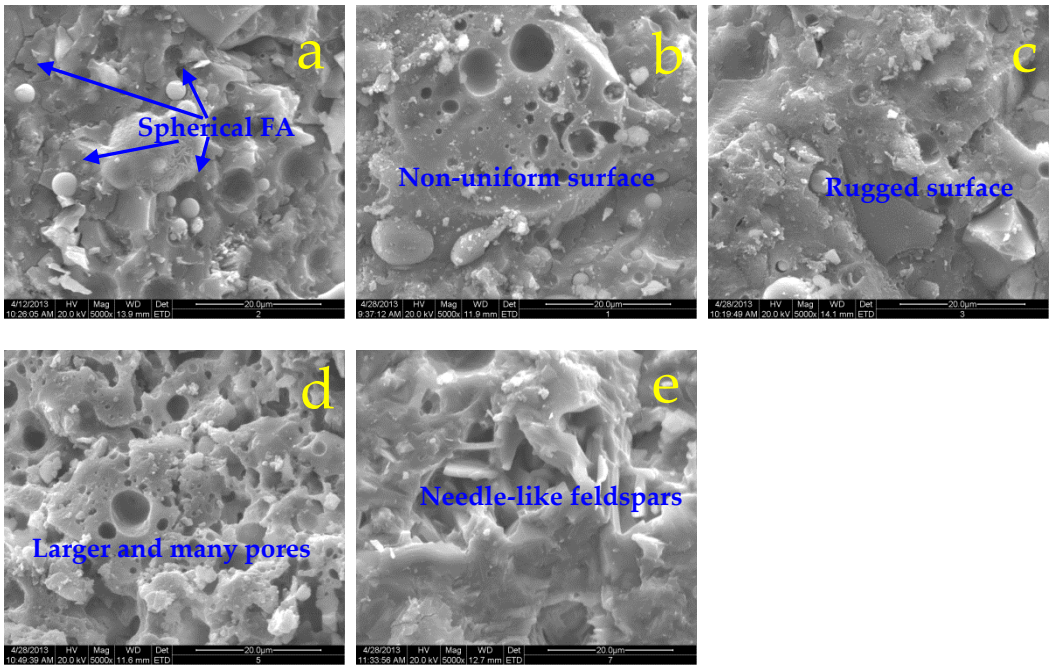

Figure 5. SEM photos of binary slag/FA binders after heat treatment. (a) RT, (b) 150°C, (c) 500°C, (d) 850°C, (e) 1200°C.

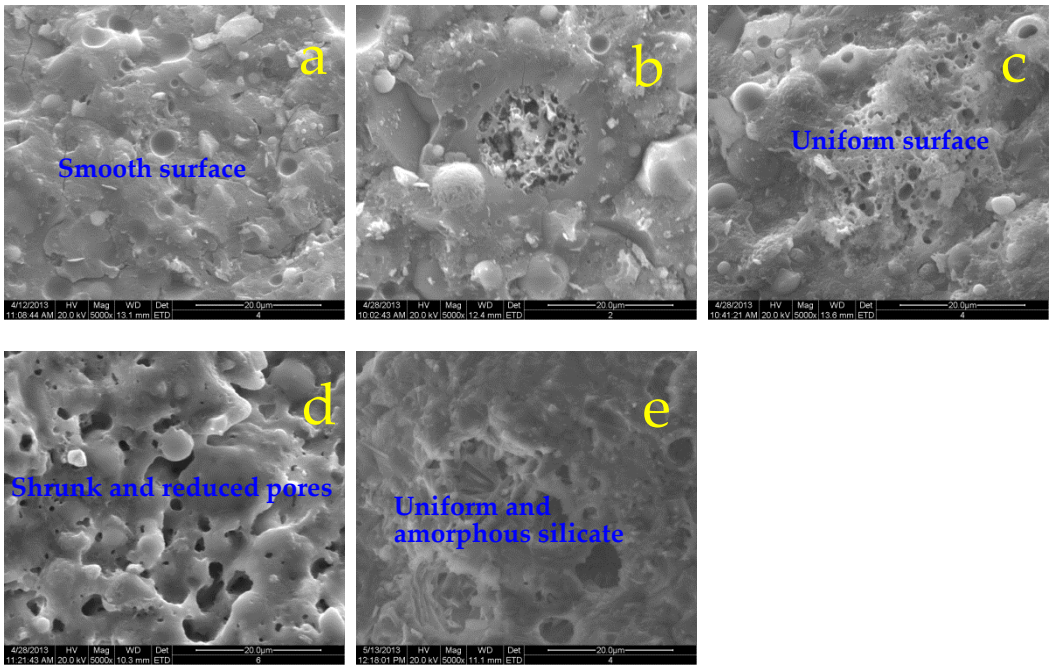

Figure 6. SEM photos of ternary SF/slag/FA binders after heat treatment. (a) RT, (b) 150°C, (c) 500°C, (d) 850°C, (e) 1200°C.

3.3.3. Pore size distributions

The replacement with 10 wt% SF favors improving the compactness of binary slag/FA pastes, the pore volume of 0.2~3 μm exerts an obvious increase as shown in Table

 doi:10.20944/preprints202305.2244.v1

2, which climbs from 11.39% to 35.81%. Because the incorporated SF could trigger the formation of N-A-S-H or N-(Ca)-A-S-H, prompting the chain propagation of geopolymer, the Ca mainly derives from the slag for balancing the charge of aluminosilicate inorganic polymers. And also the unreacted SF insert or fill the interstices of the N-A-S-H, making the porosity drop from 20.93% to 13.47%, and the median pore diameter decreases from 6.4 to 5.6 nm. Combining with the images of SEM in Fig.5a and Fig.6a, it confirms again that the incorporated SF plays an effective and crucial role in reinforcing the microstructure of slag/FA pastes, leading to the compact and dense structure.

Table 2. Pore size distributions of specimens at RT

Specimens	<20nm (%)	20-200nm (%)	0.2~3μm (%)	>3μm (%)	Median pore diameter (nm)	Porosity (%)
Slag/FA paste	40.02	9.17	11.39	38.43	6.4	20.93
SF/slag/FA paste	41.16	3.14	35.81	19.88	5.6	13.47

3.4. TG/DTG and DSC

The TG/DTG and heat flow curves of specimens are shown in Fig.7, the peak shifts from 128°C to 135°C after the replacement of FA with 10 wt% SF from the DTG curve, corresponding to the higher thermal stability. Meanwhile, the end temperature of mass loss rises from 166 to 185°C from the TG in Fig.7a-b, indicating higher thermal stability. Because of the pozzolan and filling effects of SF, which could react with the N-A-S-H or N-(Ca)-A-S-H to form more gels, and also it could insert or fill the space left by the geopolymerization [8-9], leading to an increase in the DTG peak.

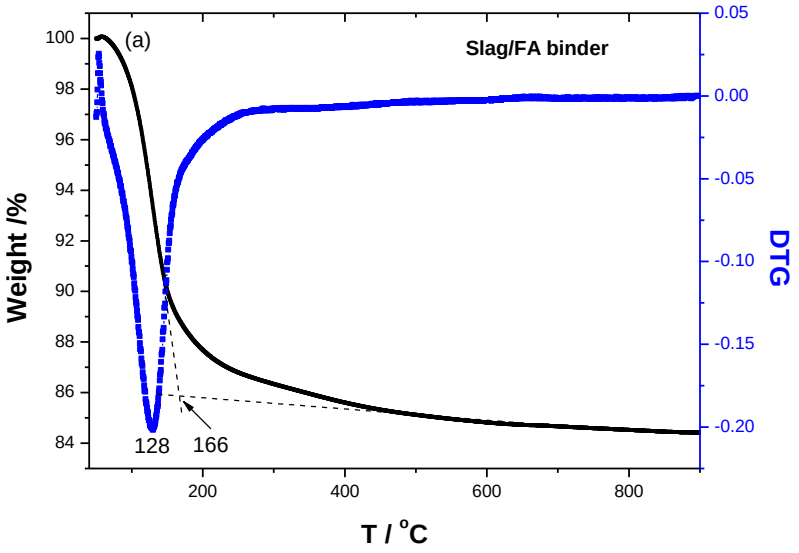

Preprints (www.preprints.org) | NOT PEER-REVIEWED | Posted: 31 May 2023 doi:10.20944/preprints202305.2244.v1

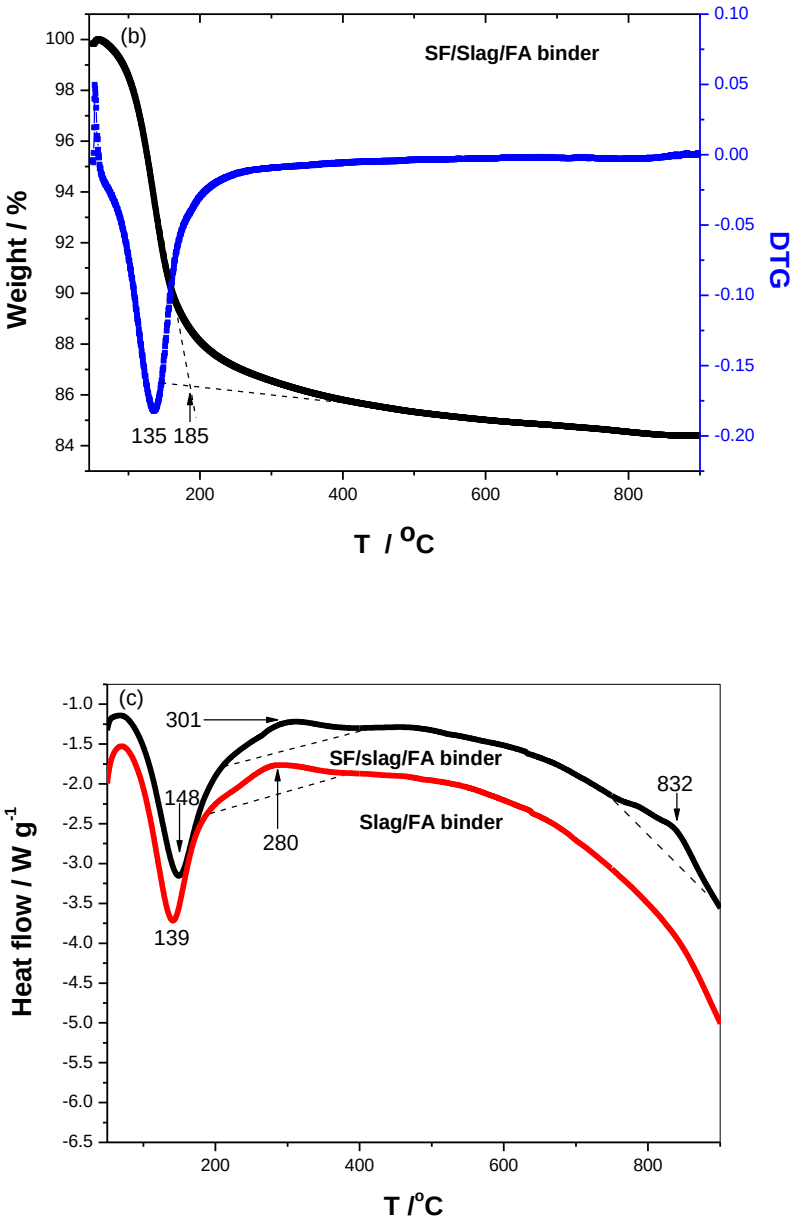

Figure 7. TG/DTG and heat flow of samples including, (a) Slag/FA paste, (b) SF/slag/FA paste, and (c) Heat flow, respectively.

The heat flow of the specimen reveals that the SF postpones the thermal exchange between the matrix and surrounding in the sub-high temperature, the endothermic peak shifts from 139 to 148°C, and the tiny exothermic peak shifts from 280 to 301°C as shown in Fig.7c. It is reported that dehydration of specimens occurs below 300°C, dehydroxylation derived from SiO_4 or AlO_4 tetrahedron occurs at about 500°C, and on the order of 900°C is required for complete decomposition of the N-(C)-A-S-H [23]. It is appropriate to emphasize that no endothermic peak at around 450°C caused by the dehydration of $Ca(OH)_2$ is detected, revealing that no $Ca(OH)_2$ formed [24]. There is no endothermic peak at around 500°C, presenting few SiO_4 or AlO_4 tetrahedrons. Interestingly, the tiny exothermic peak at 832°C might be attributed to the melting of amorphous silicates involved in geopolymer.

Preprints (www.preprints.org) | NOT PEER-REVIEWED | Posted: 31 May 2023 doi:10.20944/preprints202305.2244.v1

3.5. FTIR analysis

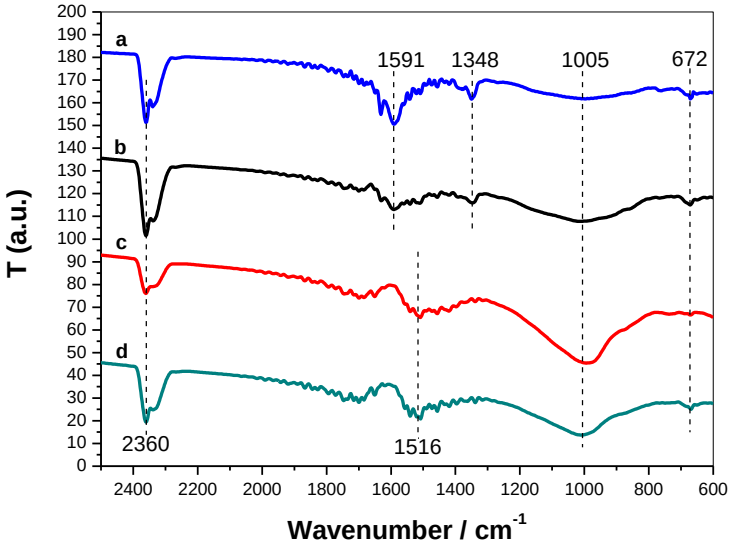

Figure 8. FTIR spectra of samples including a-SF/slag/FA binder after 1200°C exposure, b-slag/FA binder after 1200°C exposure, c-slag/FA binder after 150°C exposure, and d- SF/slag/FA binder after 150°C exposure, respectively.

The peak at 1005 cm^{-1} is assigned to the oligomeric Si-O vibration [25], which shifts to a lower wavenumber after the incorporation of SF, due to the increasing content of monomeric $Si(OH)_4$ as shown in Fig.8c-d. The absorption peak at 2360 cm^{-1} is attributed to the environment, and the new peak at 1348 cm^{-1} is assigned to the vibration of $[SiO_4]^{4-}$ and $[AlO_4]^{5-}$[26]. The peak at 672 cm^{-1} is associated with Si-O-Al stretching vibrations [27]. The reactive Si-OH in the N-A-S-H or N-(Ca)-A-S-H chains dehydrates and transforms into silicates. Similarly, the combination reactions between $[SiO_4]^{4-}$ and $[AlO_4]^{5-}$ occur during the heat treatment of 1200°C, corresponding to the formation of gehlenite and labradorite, combining with the results of XRD and SEM.

4. Discussions

4.1.Mechanical strength and elevated temperatures

During the sub-high temperature, the pozzolan and filling effects of SF could promote the formation and transformation of amorphous silicates within the binary slag/FA binder, which is beneficial for improved strength. The amorphous SiO_2 involved in the SF is a typical forming agent of the network, the enrichment of $Si(OH)_4$ accelerates the forming of a silicate network by extending ≡Si-O-Si≡ chains and creating bridging oxygen groups, which could trap the Ca^{2+} for charge equilibrium. Actually, a moderate temperature treatment (⩽100 °C) may enhance the tensile properties of FA/cement binder due to the formation of more micro-cracks [28].

When the temperature is above 800 °C, the mechanical strength of specimens suffers a dramatic drop. It is in agreement with Su [29], implying that the heat treatment at about 800 °C is fatal for geopolymers. On the other hand, replacement with 10 wt% SF lowers the CaO/SiO_2 and Al_2O_3/SiO_2 molar ratios, which drop from 0.325 and 0.638 to 0.297 and 0.528 (SF-containing sample) according to the chemical composition, respectively. The SF-containing sample exerts a lower melting point and a higher volume deformation at 1200°C. Wu et al. [30] suggest that lower CaO/SiO_2 and Al_2O_3/SiO_2 could enhance the viscosity in the system of SiO_2-Al_2O_3-CaO-MgO-Na_2O-K_2O. A lower melting point induced by substitution with 10wt% SF promotes the increasing content of silicate melts, which

 doi:10.20944/preprints202305.2244.v1

could "seal" the cracks, improving the temperature-induced dehydration, dehydroxylation, and thermal incompatibility [31], as well as the stress induced by varying degrees of shrinkage within matrix during the cooling process [32].

4.2. Microstructure and elevated temperatures

Because the dehydration of calcium silicate hydrate (C-S-H) occurs at 135–150°C[33], the doped SF could react with binary slag/FA binder and transform into N-A-S-H or N-(Ca)-A-S-H, leading to a denser and compact micro-structure, presenting a right shift of endothermic peak form the result of DTG, as well as increases in the mechanical properties. Meanwhile, an empirical relationship between the flexural strength and porosity (p) is shown in equation (1), where σ_0 and n are two constants determined experimentally [34]. It follows that the flexural strength decreases exponentially with porosity. The replacement of FA with SF favors a lower porosity and an increase in the pore volume of 0.2~3μm, as well as the retardance of water evaporation due to denser structures [35].

$$\sigma_{FS} = \sigma_0 \bullet \exp(-np) \tag{1}$$

During the heat treatment of sub-high temperature, the mechanical strength is improved due to the further geopolymerization within the slag/FA paste, with "right shifts" of mass loss peak and the endothermic peak of heat flow, leading to the denser and smooth fracture surface of microscopic morphology.

Because the SF begins to fuse at 1100 °C and forms a viscous liquid phase [36]. However, when the specimen is exposed to 1200°C heat treatment for 2h, the melting of the amorphous silicates at 1000~1100°C occurs, which boosts the bloating effect within the matrix. While the specimen without SF appears little melt, because of the tension induced by the escaping O_2, which promotes more cracks and accelerates a fast deterioration of the matrix, corresponding to the lower flexural strength. Tsai et al. [37] find that bloating effect occurs in municipal solid waste, and our finding is the amorphous SF diminishes the melting point, boosting the reactions between $[SiO_4]^{4-}$ and $[AlO_4]^{5-}$ and the formation of labradorite. As a kind of phase change material, the bloating SF holds beneficial effects of crack blunting and twisting [38] as a liquid phase.

On the whole, SF plays a strengthening role in the slag/FA paste due to the filling effect and pozzolan reactivity during the sub-high temperature. The filling effect could insert the gap or holes and form micro-cracks, and pozzolan reactivity promotes more amorphous gels through further geopolymerization, which favors the increasing pore volume of 0.2~3μm, resulting in a continuous increase in the mechanical strength, favoring "right shifts" of endothermic peak and the initial and final temperature of mass loss, presenting uniform and smooth fracture surface. Meanwhile, during the heat treatment above 850°C, the substitution of FA with 10 wt% SF diminishes the melting point of binary slag/FA binder, the unreacted SF is prone to melt and transforms into a liquid phase, which could generate crack blunting and twisting, leading to the occurrence of bloating effect with a greater volume deformation, promoting the formation of labradorite between $[SiO_4]^{4-}$ and $[AlO_4]^{5-}$ involved in the geopolymer chains, evidenced by the results of XRD.

5. Conclusions

The effect of silica fume on the microstructure of alkali-activated slag/FA (slag: FA=30:70, wt.%) pastes after exposure to the elevated temperatures (150, 500, 850, and 1200°C) is investigated by XRD, SEM, TG, MIP, and FTIR spectroscopy. It determines that adjusting the solid-waste formulation could improve geopolymer's fireproof performance, the following conclusions are drawn.

(1) Due to the filling and pozzolan effect, the replacement of FA with 10 wt% SF promotes the increasing pore volume of 0.2~3μm during the sub-high temperature below 850°C, leading to a continuous increase in the mechanical strength, "right shifts" of endothermic peak, appearing uniform and compact fracture surface.

 doi:10.20944/preprints202305.2244.v1

(2) The transformation of gehlenite and labradorite occurs for the samples after exposure to the elevated temperature above 850℃. And the bloating effect occurs involved in the unreacted SF altogether with the amorphous N-A-S-H or N-(Ca)-A-S-H at 1200℃, leading to a greater deformation, due to the further restructuring of the geopolymer chain composed from the $[SiO_4]^{4-}$ and $[AlO_4]^{5-}$ tetrahedra.

Acknowledgments: None.

References

[1] Wang S, Liu B, Zhang Q, et al. Application of geopolymers for treatment of industrial solid waste containing heavy metals: State-of-the-art review. Journal of Cleaner Production 390 (2023) 136053.

[2] Harmal A, Khouchani O, El-Korchi T, et al. Bioinspired brick-and-mortar geopolymer composites with ultra-high toughness. Cement and Concrete Composites 137 (2023) 104944.

[3] Peng X, Li H, Hu Y. Preparation of metakaolin-fly ash cenosphere based geopolymer matrices for passive fire protection. Journal of Materials Research and Technology 23 (2023) 604-610.

[4] Raut A, Murmu A, Alomayri T. Physico-Mechanical and thermal behavior of prolong heat Cured geopolymer blocks. Construction and Building Materials 370 (2023) 130309.

[5] Oh J, Monteiro P, Jun S, et al. The evolution of strength and crystalline phases for alkali-activated ground blast furnace slag and fly ash-based geopolymers. Cement and Concrete Research 40 (2010) 189–196.

[6] Luo X, Xu J, Bai E, et al. Systematic study on the basic characteristics of alkali-activated slag-fly ash cementitious material system. Construction and Building Materials 29 (2012) 482–486.

[7] Chithiraputhiran S, Neithalath N. Isothermal reaction kinetics and temperature dependence of alkali activation of slag, fly ash and their blends. Construction and Building Materials 45 (2013) 233–242.

[8] Danish A, Oz A, Bayrak B, et al. Performance evaluation and cost analysis of prepacked geopolymers containing waste marble powder under different curing temperatures for sustainable built environment. Resources, Conservation & Recycling 192 (2023) 106910.

 doi:10.20944/preprints202305.2244.v1

[9] Hossein H, Hamzawy E, El-Bassyouni G, et al. Mechanical and physical properties of synthetic sustainable geopolymer binders manufactured using rockwool, granulated slag, and silica fume. Construction and Building Materials 367 (2023) 130143.

[10] Rovnaník P, Bayer P, Rovnaníková P. Characterization of alkali activated slag paste after exposure to high temperatures. Construction and Building Materials 47 (2013) 1479–1487.

[11] Rashad A, Bai Y, Basheer P, et al. Chemical and mechanical stability of sodium sulfate activated slag after exposure to elevated temperature. Cement and Concrete Research 42 (2012) 333–343.

[12] Rashada A, Khalil M. A preliminary study of alkali-activated slag blended with silica fume under the effect of thermal loads and thermal shock cycles. Construction and Building Materials 40 (2013) 522–532.

[13] Shilar F, Ganachari S, Patil V, et al. Preparation and validation of sustainable metakaolin based geopolymer concrete for structural application. Construction and Building Materials 371 (2023) 130688.

[14] Bernardo E, Dal Maschio R. Glass–ceramics from vitrified sewage sludge pyrolysis residues and recycled glasses. Waste Management 31 (2011) 2245–2252

[15] Bernardo E, Esposito L, Rambaldi E, et al. Sintered esseneite–wollastonite–plagioclase glass–ceramics from vitrified waste. Journal of the European Ceramic Society 29 (2009) 2921–2927.

[16] Segui P, Aubert J, Husson B, et al. Utilization of a natural pozzolan as the main component of hydraulic road binder. Construction and Building Materials 40 (2013) 217–223

[17] Bernardo E, Bonomo E, Dattoli A. Optimisation of sintered glass–ceramics from an industrial waste glass. Ceramics International 36 (2010) 1675–1680

[18] Fang Y, Kayali O. The fate of water in fly ash-based geopolymers. Construction and Building Materials 39 (2013) 89–94

[19] Yilmaz G. Structural characterization of glass–ceramics made from fly ash containing SiO2–Al2O3–Fe2O3–CaO and analysis by FT-IR–XRD–SEM methods. Journal of Molecular Structure 1019 (2012) 37–42

 doi:10.20944/preprints202305.2244.v1

[20] Rathossi C, Pontikes Y. Effect of firing temperature and atmosphere on ceramics made of NW Peloponnese clay sediments. Part I: Reaction paths, crystalline phases, microstructure and colour. Journal of the European Ceramic Society 30 (2010) 1841–1851.

[21] Ding J, Ma S, Zheng S, et al. Study of extracting alumina from high-alumina PC fly ash by a hydro-chemical process. Hydrometallurgy 161 (2016) 58–64

[22] Sarıdemir M, Çelikten S. Effects of Ms modulus, Na concentration and fly ash content on properties of vapour-cured geopolymer mortars exposed to high temperatures. Construction and Building Materials 363 (2023) 129868.

[23] Guerrieri M, Sanjayan J. Behavior of combined fly ash/slag-based geopolymers when exposed to high temperatures. Fire Mater. 2010, 34:163–175.

[24] Rashad A, Sadek D, Hassan H. An investigation on blast-furnace slag as fine aggregate in alkali-activated slag mortars subjected to elevated temperatures. Journal of Cleaner Production, 2016, 112: 1086–1096.

[25] Hua S, Yan W, Duan J. Polymerization of silicate on TiO2 and its influence on arsenate adsorption: An ATR-FTIR study. Colloids and Surfaces A: Physicochem. Eng. Aspects 469 (2015) 180–186

[26] Penilla R, Bustos A, Elizalde S. Zeolite synthesized by alkaline hydrothermal treatment of bottom ash from combustion of municipal solid wastes [J]. Journal of the American Ceramic Society, 2003, 86: 1527−1533

[27] Bai Y, Guo W, Zhao Q, et al. Performance deterioration of municipal solid waste incineration fly ash-based geopolymer under sulfuric acid attack. Construction and Building Materials, 391 (2023) 131847.

[28] Yu J, Lin J, Zhang Z, et al. Mechanical performance of ECC with high-volume fly ash after sub-elevated temperatures. Construction and Building Materials, 2015,99: 82–89.

[29] Su H, Xu J, Ren W. Mechanical properties of geopolymer concrete exposed to dynamic compression under elevated temperatures. Ceramics International, 2016,42: 3888–3898.

[30] Wu G, Yazhenskikh E, KlausHack E, et al. Viscosity model for oxide melts relevant to fuel slags. Part 1: Pure oxides and binary

 doi:10.20944/preprints202305.2244.v1

systems in the system SiO2–Al2O3–CaO–MgO–Na2O–K2O. Fuel Processing Technology 137 (2015) 93–103

[31] Zhang H, Kodur V, Wu B, et al. Thermal behavior and mechanical properties of geopolymer mortar after exposure to elevated temperatures. Construction and Building Materials, 2016,109:17-24.

[32] Ren X, Zhang W, Zhang Y, et al. Effects of Fe2O3 content on microstructure and mechanical properties of CaO−Al2O3−SiO2 system. Trans. Nonferrous Met. Soc. China 25(2015) 137−145

[33] Rong Z, Sun W, Xiao H, et al. Effects of nano-SiO2 particles on the mechanical and microstructural properties of ultra-high performance cementitious composites. Cement & Concrete Composites 56 (2015) 25–31

[34] Zhao X, Zhang N, Ru H, et al. Mechanical properties and toughening mechanisms of silicon carbide nano-particulate reinforced Alon composites. Materials Science and Engineering A 538 (2012) 118– 124

[35] Zhang Y, Wang Y, Xu D, et al. Mechanical performance and hydration mechanism of geopolymer composite reinforced by resin. Materials Science and Engineering A527 (2010) 6574–6580

[36] Xu J, Zhao F, Guo Q, et al. Characterization of the melting behavior of high-temperature and low-temperature ashes. Fuel Processing Technology 134 (2015) 441–448

[37] Tsai C, Wang K, Chiou I. Effect of SiO2–Al2O3–flux ratio change on the bloating characteristics of lightweight aggregate material produced from recycled sewage sludge. Journal of Hazardous Materials B134 (2006) 87–93

[38] Fernandes F, Manari S, Aguayo M, et al. On the feasibility of using phase change materials (PCMs) to mitigate thermal cracking in cementitious materials. Cement & Concrete Composites 51 (2014) 14–26